



Biogas reforming for syngas production: The effect of methyl chloride



McKenzie P. Kohn, Marco J. Castaldi*, Robert J. Farrauto

Earth and Environmental Engineering Department, HKSM, Columbia University in the City of New York, 500 West 120th Street, New York, NY 10027, USA

ARTICLE INFO

Article history:

Received 11 February 2013

Received in revised form 13 June 2013

Accepted 12 July 2013

Available online 21 July 2013

Keywords:

Biogas

Reforming

Syngas

Rhodium

Methyl chloride

ABSTRACT

Biogas is a mixture of primarily methane and carbon dioxide produced from the anaerobic microbial digestion of biomass. A 4% Rh/Al₂O₃ catalyst was investigated for its ability to reform biogas in the presence of a chloride impurity, specifically CH₃Cl that is often found in biogas systems. The conditions tested included temperatures between 350 °C and 700 °C with CH₃Cl concentrations between 0 and 200 ppm at atmospheric pressure and 1050 h⁻¹ WHSV. It was determined that in the dry reforming reaction CH₃Cl reacts with the alumina support to produce surface chloride which increases the surface acidity and reversibly poisons the reverse water–gas shift reaction. For example, with the addition of 50 ppm CH₃Cl the H₂/CO ratio increased by 40% at 350 °C and by 2% at 700 °C. All changes were reversible upon removal of CH₃Cl from the feed. Furthermore, less surface chloride was observed using XPS at 700 °C compared to 400 °C, and the effect on selectivity decreased with CH₃Cl concentrations less than 50 ppm. Therefore the degree of chloride poisoning is directly proportional to CH₃Cl concentration and inversely proportional to temperature.

© 2013 Elsevier B.V. All rights reserved.

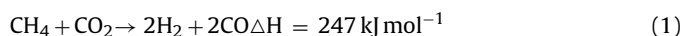
1. Introduction

Biogas is a mixture of methane and carbon dioxide produced from the anaerobic microbial digestion of biomass. The gas is often produced in landfills, agricultural operations, and in wastewater treatment plants. Biogas from landfills alone is the second largest source of anthropogenic methane emissions in the United States, producing 13.5 billion m³ of methane per year [1]. In the U.S. only 18% of landfill gas is used for energy [2,3] because the high CO₂ content decreases the heating value and flame stability of the gas mixture. This leads to increased CO, NO_x, and unburned hydrocarbon emissions when the gas is combusted in an engine, turbine, or boiler compared to pure CH₄ or natural gas [4]. Therefore biogas is often flared without extracting any of the latent chemical energy.

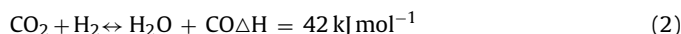
Catalytic dry reforming of biogas (Eq. (1)) has the potential to fully utilize the energy contained in the biogas by converting both the CH₄ and CO₂ into H₂ and CO, or syngas [5]. Syngas is valuable because it can be used as a combustion enhancer due to its high reactivity [4], which decreases the emissions associated with combusting the biogas, or as a precursor for liquid fuels or fuel cells [6]. Dry reforming is usually accompanied by the reverse water–gas shift reaction (Eq. (2)) that decreases the H₂/CO ratio to a value slightly less than one in the temperature range of 400–800 °C. In

this work a Rh/Al₂O₃ catalyst is used because it is less susceptible to carbon formation during dry reforming which can deactivate the catalyst compared to base metals such as nickel [7].

Dry Reforming



Reverse Water–Gas Shift

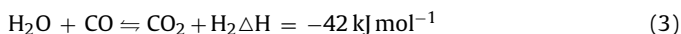


One problem with catalytically reforming biogas is the trace amounts of sulfur and chlorinated compounds present that could potentially poison the catalyst. The effect of sulfur compounds on reforming catalysts has been widely studied because sulfur is commonly present in oil and its derivatives such as gasoline [6]. Chlorocarbons are not as widely studied although they are present in biogas [8,9], as well as in the gasification and combustion products of biomass, coal, and municipal solid waste [10–13] in amounts similar to sulfur compounds (10–50 ppm) [8]. The chlorocarbons originate from the natural presence of chlorinated compounds in organic material that are released during decomposition, gasification or combustion of organic material. Therefore as the production of bio-derived fuels increases, the effect of chlorocarbons on reforming catalysts will become more important. CH₃Cl, the simplest chlorocarbon and most abundant atmospheric halocarbon, is used as the chlorocarbon surrogate in this work to investigate the effect of 10–50 ppm of a chlorinated compound on the activity and selectivity of the dry reforming reaction over the Rh/γAl₂O₃ catalyst.

* Corresponding author. Present address: Chemical Engineering Department, Grove School of Engineering, City College of New York, 140th Street and Convent Avenue, Steinman Hall, Room 307, New York, NY 10031, USA. Tel.: +1 212 650 6679. E-mail address: mcastaldi@che.cuny.cuny.edu (M.J. Castaldi).

While the effect of CH_3Cl on the dry reforming reaction has not been previously studied, steam reforming of various chlorocarbons over base and precious metal catalysts supported on $\gamma\text{Al}_2\text{O}_3$ has been studied. Richardson et al. [14–22] found that for a variety of chlorocarbons, chloride adsorption on the catalyst poisons the forward water–gas shift reaction, Eq. (3), but not the chlorocarbon steam reforming activity, shown for CH_3Cl in Eq. (4).

Water–Gas Shift



CH_3Cl Steam Reforming:



The most active catalysts for the steam reforming reaction were Rh, Pt, and Pd followed by Cu, Re, Ir, Ru, Ni, and then Co, in decreasing activity. On the precious metal catalysts carbon formation occurred to some extent but was not a major cause for activity loss. Experiments with both CH_3Cl and CH_4 suggested that the two species may compete for reforming sites and that CH_3Cl reacts preferentially. On all catalysts supported on alumina, a loss in water–gas shift activity was observed via an increase in CO and a decrease in CO_2 at temperatures lower than 700°C [17]. Chlorocarbon steam reforming experiments on a Pt/ ZrO_2 catalyst, however, did not exhibit water–gas shift poisoning, while the chlorocarbon reforming activity remained high and close to equilibrium [22], showing a sensitivity to the catalyst support.

After the chlorocarbon steam reforming experiments, regeneration of the water gas shift (WGS) activity using H_2O was possible. To explain these results, it was suggested that chloride replaces alumina hydroxyl sites that are in equilibrium with steam. By replacing these alumina hydroxyl (OH) sites, chloride poisons the WGS reaction which is also dependent on these OH sites. The replacement of alumina hydroxyl groups by chloride is supported by other work showing that on a working alumina catalyst, in which a mixture of Lewis acid, Brønsted acid, and basic sites exist, HCl can dissociate on the catalytic acid–base pairs to form Al-Cl and H_2O [23]. The net reaction is a replacement of one alumina hydroxyl group with a chloride as shown in Eq. (5) [24,25]. The net reaction clarifies the role of the H_2O gas concentration for keeping the alumina surface free of chloride.



The replacement of a hydroxyl group, which in most configurations is basic, increases the acidity of the alumina [26]. The presence of the chloride also polarizes the lattice of hydroxyl groups and weakens the remaining O–H bonds [26,27], increasing the Brønsted acidity of the alumina. The effect of chloride adsorption on support acidity is well known in the field of naphtha reforming in which chlorocarbons are supplied to maintain the acidity of a Pt/ Al_2O_3 or Pt-Re/ Al_2O_3 catalyst [6]. The increased support acidity affects the water gas shift reaction which is dependent on the basicity of the support, originating primarily from the alumina hydroxyl (OH) groups, to produce the necessary formate or carbonate intermediates [28–33] to proceed in either the forward or reverse direction.

2. Experimental methods

2.1. Catalyst preparation

A 4% Rh/ $\gamma\text{Al}_2\text{O}_3$ catalyst, obtained from BASF Catalysts, was used for all of the experimental work presented here. The catalyst was prepared using a rhodium nitrate solution so that any chloride present on the catalyst originated from the reaction conditions and not the preparation technique. The powder catalyst was prepared by ball milling the impregnated catalyst to an average

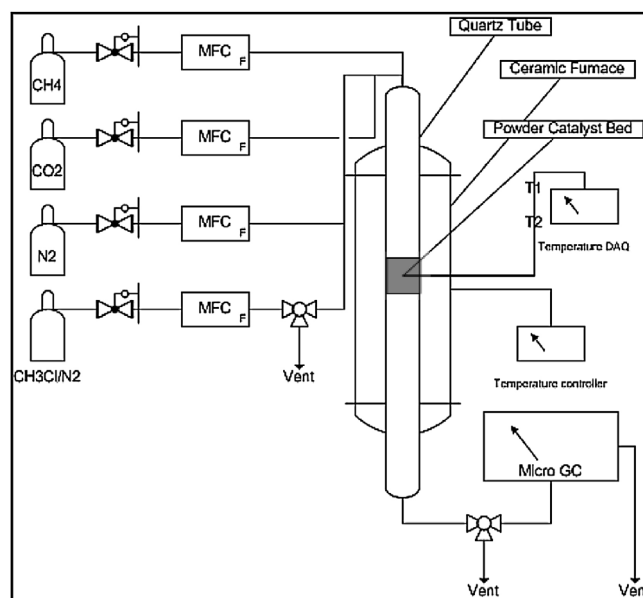


Fig. 1. Schematic of flow-through reactor apparatus (not to scale).

particle size of $10 \mu\text{m}$. The density of the 4% Rh/ Al_2O_3 powder was 0.84 g/cm^3 . The catalyst was calcined in air at 725°C . The BET specific surface area of the calcined catalyst powder was $110 \text{ m}^2/\text{g}$, measured using a Quantachrome Nova 2200e. The dispersion of the Rh metal was 40%, measured using CO chemisorption with a thermo-gravimetric analyzer (Netzsch, STA 409 PC Luxx) assuming a 1:1 CO:Rh adsorption ratio. The mean particle size, calculated using the 40% dispersion value, was 2.7 nm , assuming Rh atom surface area = 7.58 \AA^2 and Rh density = 12.4 g/cm^3 [34].

2.2. Flow-through reactor

Flow-through reactor experiments were performed in a quartz reactor (Fig. 1) operated at 1 atm pressure and temperatures between 350°C and 700°C . The quartz tube had an inner diameter of 1.905 cm and length of 30.5 cm . 0.15 g of 4% Rh/ Al_2O_3 powder composed the catalyst bed, resulting in a bed size of 1.905 cm diameter and 0.09 cm length. The flow rate of the reactant gases was $2100 \text{ ml}\cdot\text{min}^{-1}$, or $2.6 \text{ g}\cdot\text{min}^{-1}$, resulting in a weight hourly space velocity (WHSV) of 1050 h^{-1} or a gas hourly space velocity (GHSV) of $705,600 \text{ h}^{-1}$ in order to reduce diffusion and mass transfer effects. UHP CH_4 , CO_2 and N_2 (Techair) were used to simulate a landfill gas. A mixture of 1000 ppm CH_3Cl in N_2 (Techair) was used to introduce CH_3Cl . The mass flow rate of each inlet gas into the reactor was controlled with mass flow controllers (Aalborg, GFC17). A tube furnace was controlled with a temperature controller (Omega, CN9000A Series) and K-type thermocouples (Omega, KMTIN Series). One thermocouple was placed upstream of the catalyst bed to measure the gas preheat temperature, and another thermocouple was placed in the catalyst bed to measure the reaction temperature.

Flow-through reactor tests were performed by exposing the 4% Rh/ Al_2O_3 powder catalyst to a target mixture of 5.5% CH_4 , 7% CO_2 in a balance of N_2 until the reactor temperature and conversion stabilized. A mixture of 1000 ppm CH_3Cl in N_2 was used to introduce CH_3Cl . The final CH_3Cl concentration was 10, 25, or 50 ppm CH_3Cl , depending on the experiment. The CH_3Cl was introduced for 1 h. CH_3Cl was then removed and the test continued to run for at least 1 h with the initial gas mixture. When CH_3Cl was introduced, the N_2 flow rate was reduced to maintain a constant flow rate.

Product species were monitored throughout the experiment with an on-line Agilent Micro GC (3000).

2.3. Catalyst characterization

XPS, acidity and basicity characterization, CO chemisorption and BET surface area measurements were performed on pre-tested Rh/Al₂O₃ powder catalyst as well as on catalyst samples that were exposed to the conditions shown in Table 1 in the flow-through reactor and then removed from the reactor for characterization. Thermo-gravimetric analysis was also performed to evaluate the effect of CH₃Cl on the catalyst in situ. CO chemisorption and BET surface area results for the pre-tested Rh/Al₂O₃ powder were presented in Section 2.1. In the following sections TGA, XPS, and acidity experimental conditions will be discussed.

2.3.1. TGA

Thermo-gravimetric analysis (Du Pont TGA, 951) was used to measure the weight change of the 4% Rh/γAl₂O₃ catalyst as a result of CH₃Cl exposure. These experiments were conducted by exposing approximately 0.018 g of the 4% Rh/γAl₂O₃ catalyst to a dry reforming mixture (5% CH₄, 6% CO₂, balance N₂) and heating to the desired reaction temperature of either 400 °C, 500 °C, 600 °C, or 700 °C. After the isotherm was reached, 200 ppm of CH₃Cl was introduced for 15 min and then turned off. The weight changes in the catalyst as a result of CH₃Cl introduction and removal were observed.

2.3.2. XPS

XPS analysis was performed using a Thermo Fisher K Alpha XPS equipped with an Al Kα monochromatic source. Fresh and used powder catalyst samples were mounted on double sided tape for analysis. The run conditions were as follows: pass energy = 40 eV, vacuum conditions were 5E-8 torr or lower. Data was analyzed using Thermo Fisher Advantage software and Scofield sensitivity factors. Binding energies were referenced to C1s = 285.0 eV.

2.3.3. Acidity characterization

Temperature programmed desorption of ammonia was used to measure the acidity of the catalyst surface and the relative strength of acid sites on the Rh/γAl₂O₃ catalyst. This characterization was performed in a thermo-gravimetric analyzer (Netzsch, STA 409 PC Luxx). The catalyst was first dried in N₂ at 150 °C for 1.5 h and then exposed to 1% NH₃ in a balance of Argon at 100 °C for 10 min. The system was then flushed with N₂ and the temperature was increased from 100 °C to 700 °C at 10 °C/min to desorb the NH₃. The derivative of weight loss during the desorption step produces a peak at which weight loss is the most rapid, attributed here to the removal of NH₃. Integration of this peak gives the amount of NH₃ desorbed in mmol g⁻¹ catalyst, and error bars on these values represent the uncertainty associated with exact onset and completion of signal from baseline during integration analysis. The acid sites measured are a sum of Lewis and Brønsted acidity. The temperature at which NH₃ desorbs is an indication of the acid strength [31].

Table 1

Experiment protocol for 4% Rh/Al₂O₃ powder samples used for characterization. WHSV = 1050 h⁻¹.

Name	Conditions	[CH ₃ Cl]	Temperature (°C)	Time (h)
400 °C, No CH ₃ Cl, 10 h	5.6% CH ₄ , 7.0% CO ₂	0	400	10
400 °C, 50 ppm CH ₃ Cl, 10 h	5.6% CH ₄ , 7.0% CO ₂	50 ppm	400	10
700 °C, No CH ₃ Cl, 3 h	5.6% CH ₄ , 7.0% CO ₂	0	700	3
700 °C, 50 ppm CH ₃ Cl, 3 h	5.6% CH ₄ , 7.0% CO ₂	50 ppm	700	3
700 °C, No CH ₃ Cl, 10 h	5.6% CH ₄ , 7.0% CO ₂	0	700	10
700 °C, 50 ppm CH ₃ Cl, 10 h	5.6% CH ₄ , 7.0% CO ₂	50 ppm	700	10

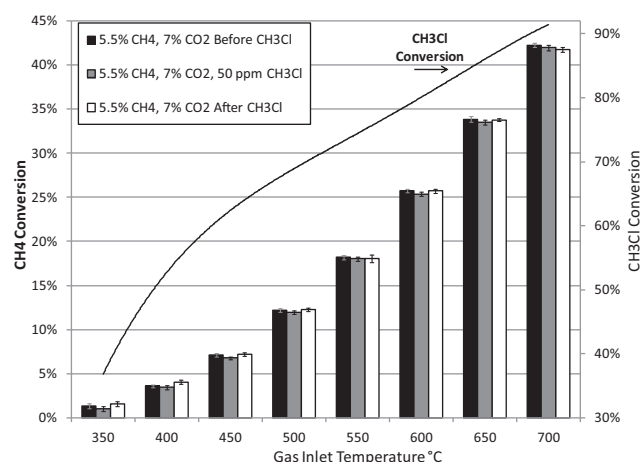


Fig. 2. CH₄ conversion as a function of temperature before, during, and after 50 ppm CH₃Cl introduction into a feed of 5.6% CH₄ and 7% CO₂ in a balance of N₂ over a 4% Rh/Al₂O₃ powder catalyst. WHSV = 1050 h⁻¹.

3. Results

3.1. Flow-through reactor

The effect of CH₃Cl on the dry reforming reaction at temperatures between 350 °C and 700 °C was investigated by introducing pulses of CH₃Cl into the reactor feed during the dry reforming reaction as explained in Section 2.2. Dry reforming activity is represented by CH₄ conversion, and selectivity is represented by the H₂/CO ratio of the product stream. Fig. 2 shows CH₄ conversion before, during, and after a 1 h pulse of 50 ppm CH₃Cl. The CH₄ conversion value is the average CH₄ conversion in the last 30 min of each 1 h segment. The error bars illustrate the standard deviation in the CH₄ conversion values during the final 30 min of each segment. Fig. 2 also shows the CH₃Cl conversion during the CH₃Cl pulse at each temperature. As seen in Fig. 2, the introduction of CH₃Cl causes a small decrease in the average CH₄ conversion value at each temperature, which is then recovered after removal of CH₃Cl. However, the changes seen as a result of CH₃Cl introduction are within the standard deviation of the CH₄ conversion values. Therefore, it is possible that CH₃Cl at higher concentrations could poison the dry reforming reaction, but this effect is not significant at 50 ppm CH₃Cl. Fig. 2 also shows that the conversion of CH₃Cl increases with temperature, reaching 91% conversion at 700 °C, showing that the CH₃Cl is undergoing reaction yet is not significantly poisoning the dry reforming reaction.

Fig. 3 shows the H₂/CO ratio of the product stream before, during, and after the 1 h pulse of 50 ppm CH₃Cl. The H₂/CO value is the average H₂/CO ratio in the last 30 min of each 1 h segment. The error bars illustrate the standard deviation in the H₂/CO ratios during the final 30 min of each segment. Importantly, regardless of CH₃Cl addition, the H₂/CO ratio decreases with temperature because the equilibrium constant for the water–gas shift reaction decreases as temperature increases, favoring H₂O and CO production over H₂ and CO₂. The introduction of CH₃Cl causes an increase in the H₂/CO

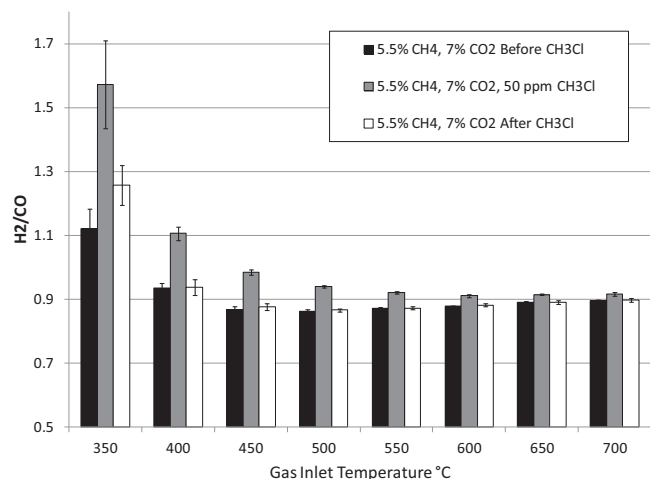


Fig. 3. H_2/CO ratio as a function of temperature before, during, and after 50 ppm CH_3Cl introduction into a feed of 5.6% CH_4 and 7% CO_2 in a balance of N_2 over a 4% Rh/Al_2O_3 powder catalyst. WHSV = $1050\ h^{-1}$.

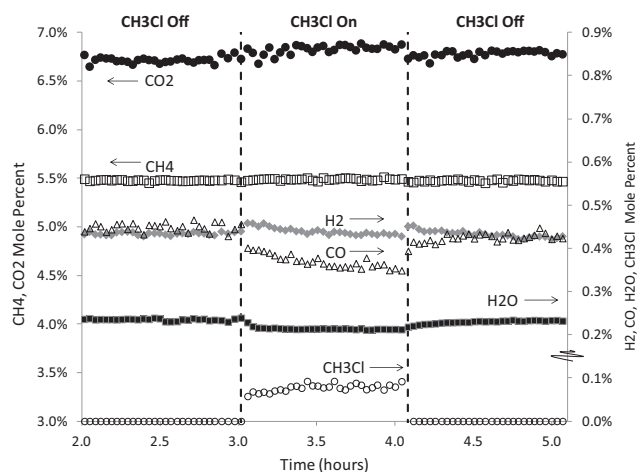


Fig. 4. The effect of 50 ppm CH_3Cl exposure for 1 hour at $400\ ^\circ C$ in a feed of 5.75% CH_4 and 7% CO_2 in a balance of N_2 on CH_4 , CO_2 , H_2 , CO , H_2O , and CH_3Cl mole percent. WHSV = $1050\ h^{-1}$.

ratio at each temperature, with the effect decreasing as temperature increases from $350\ ^\circ C$ to $700\ ^\circ C$. At each temperature except for $350\ ^\circ C$, once CH_3Cl is removed, the H_2/CO ratio returns to its previous value.

The cause for the change in H_2/CO ratio is more easily examined by observing the mole species data as a function of time. Because the changes are the most pronounced at low temperatures, mole concentrations at $400\ ^\circ C$ are used as an example. Fig. 4 and Table 2 show the effect of a one hour pulse of 50 ppm CH_3Cl at $400\ ^\circ C$ on CH_4 , CO_2 , H_2 , CO , H_2O , and CH_3Cl mole concentrations. Table 2 gives exact values for CH_4 , H_2 , CO , H_2O , CO_2 , and H_2/CO ratio at the times indicated in the first column. The error values indicate the standard

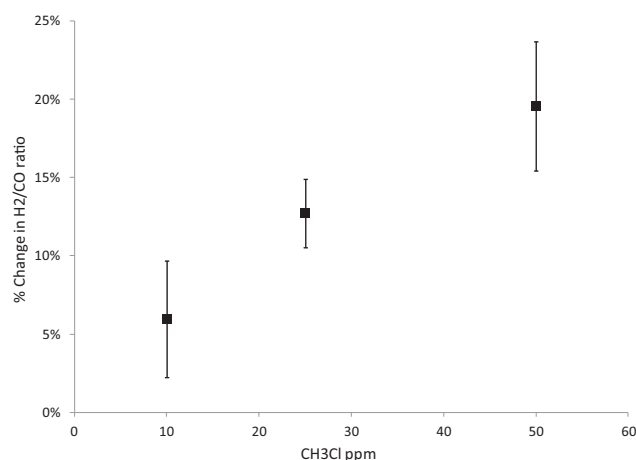


Fig. 5. Percent change in H_2/CO ratio due to CH_3Cl introduction into a feed of 5.5% CH_4 and 7% CO_2 in a balance of N_2 over a 4% Rh/Al_2O_3 powder catalyst at $400\ ^\circ C$ as a function of CH_3Cl concentration. WHSV = $1050\ h^{-1}$. Values indicate average of two (10 ppm, 25 ppm) or three (50 ppm) experiments on fresh catalyst beds; error bars indicate standard deviation between experiments.

deviation of the gas concentrations in the one hour segment before CH_3Cl introduction, when temperature and gas concentration was constant.

Fig. 4 shows that before the CH_3Cl is introduced, concentrations of CH_4 , CO_2 , H_2 , CO , and H_2O are stable. CH_4 conversion is 4.68%, syngas production ($H_2 + CO$) is 0.88%, and the H_2/CO ratio is 1.00. The presence of H_2O indicates that the reverse water–gas shift reaction is active. At 3.06 h, 50 ppm CH_3Cl is introduced, which causes an increase in CO_2 and H_2 and a decrease in CO and H_2O concentration and an increase in the H_2/CO ratio of the syngas to 1.15. Throughout the remainder of the CH_3Cl injection, CH_4 , CO_2 , and H_2O concentrations remain stable while syngas production decreases to 0.78% and H_2/CO ratio increases to 1.23. The CH_3Cl conversion during the pulse is 69%. After the CH_3Cl is removed, the syngas production increases to 0.84% while the H_2/CO ratio decreases to its pre- CH_3Cl value of 1.00. The CO_2 and H_2O concentration also return to their pre- CH_3Cl values, while CH_4 concentration remains unchanged.

In addition to 50 ppm CH_3Cl , 25 ppm and 10 ppm concentrations of CH_3Cl were tested for their effect on the activity and selectivity of the dry reforming reaction. The lower concentrations of CH_3Cl did not produce a significant enough difference to measure any change in the dry reforming activity, as observed with 50 ppm CH_3Cl . However, changes in the selectivity, as illustrated by the H_2/CO ratio, were evident. These results at $400\ ^\circ C$ are shown in Fig. 5, illustrating the percent change in H_2/CO ratio due to the CH_3Cl pulse as a function of CH_3Cl concentration. At all three concentrations, the presence of CH_3Cl caused a reversible increase in the H_2/CO ratio, similar to the results shown in Fig. 3. Furthermore, the lower the CH_3Cl concentration, the smaller the change in H_2/CO ratio. Therefore the effect of CH_3Cl on the reverse water–gas shift reaction is directly proportional to the CH_3Cl concentration.

Table 2
The effect of 50 ppm CH_3Cl exposure at $400\ ^\circ C$ in a feed of 5.75% CH_4 and 7% CO_2 in a balance of N_2 at WHSV = $1050\ h^{-1}$ on CH_4 , H_2 , CO , H_2O , and CO_2 mole percent, and H_2/CO ratio.

Condition	CH_4	H_2	CO	H_2O	CO_2	H_2/CO ratio
Before CH_3Cl (2.98 h)	$5.48 \pm 0.01\%$	$0.44 \pm 0.01\%$	$0.44 \pm 0.01\%$	$0.24 \pm 0.00\%$	$6.79 \pm 0.03\%$	1.00 ± 0.02
Immediately after CH_3Cl (3.06 h)	$5.48 \pm 0.01\%$	$0.46 \pm 0.01\%$	$0.40 \pm 0.01\%$	$0.23 \pm 0.00\%$	$6.83 \pm 0.03\%$	1.15 ± 0.02
1 h with CH_3Cl (4.00 h)	$5.49 \pm 0.01\%$	$0.43 \pm 0.01\%$	$0.35 \pm 0.01\%$	$0.21 \pm 0.00\%$	$6.83 \pm 0.03\%$	1.23 ± 0.02
1 h after CH_3Cl removed (5.00 h)	$5.48 \pm 0.01\%$	$0.42 \pm 0.01\%$	$0.42 \pm 0.01\%$	$0.23 \pm 0.00\%$	$6.76 \pm 0.03\%$	1.00 ± 0.02

Table 3

Peak binding energies (eV) determined for Al, C, Cl, O, and Rh for each of the catalyst samples.

XPS peak	400 °C No CH ₃ Cl 10 h	400 °C 50 ppm CH ₃ Cl 10 h	700 °C No CH ₃ Cl 3 h	700 °C 50 ppm CH ₃ Cl 3 h	700 °C No CH ₃ Cl 10 h	700 °C 50 ppm CH ₃ Cl 10 h
Al2p _A	74.3	74.4	74.2	74.3	74.2	74.3
C1s _A	284.7	284.8	284.6	284.8	284.7	284.8
C1s _B	286.1	286.4	285.9	286.4	286.2	286.2
C1s _C	288.4	288.8	288.2	288.4	288.4	288.4
Cl2p _A	NA	199.0	NA	198.6	NA	198.7
O1s _A	531.3	531.4	531.3	531.4	531.2	531.3
Rh3d5 _A	308.3	307.8	308.2	308.1	307.9	308.0
Rh3d5 _B	309.8	309.8	309.7	309.8	309.4	309.6

The effect of HCl on the reverse water–gas shift reaction was also explored in an attempt to separate the effects of the chloride from the CH₃ group in the CH₃Cl, and to gain insight into the CH₃Cl decomposition mechanism. A 50 ppm HCl pulse into the dry reforming reaction at 400 °C caused a change in the H₂/CO ratio of 26 ± 4%. As shown in Fig. 5, a 50 ppm pulse of CH₃Cl at 400 °C increased the H₂/CO ratio by 20 ± 4%. At 700 °C (not shown) a 50 ppm pulse of CH₃Cl increased the H₂/CO ratio by approximately 1.5%, while a 50 ppm pulse of HCl increased the H₂/CO ratio by approximately 2%. Therefore the effect of HCl on the H₂/CO ratio was similar to the effect of CH₃Cl at both 400 °C and 700 °C.

3.2. TGA

Thermo-gravimetric analysis was also performed to evaluate the effect of CH₃Cl on the catalyst in situ. 200 ppm 15 min CH₃Cl pulses were introduced to the catalyst at isotherms of 400 °C, 500 °C, 600 °C, and 700 °C as described in Section 2.3.1. At each temperature, introduction of CH₃Cl caused an immediate increase in catalyst mass and removal of CH₃Cl caused a more gradual decline in catalyst mass, with the final mass coming to equilibrium approximately 2 h after introduction of the CH₃Cl. Fig. 6 shows the weight gain of the catalyst due to CH₃Cl introduction, the weight loss of the catalyst after CH₃Cl is removed, calculated by subtracting the catalyst mass 2 h after CH₃Cl introduction from the catalyst mass immediately after the 15 min CH₃Cl pulse. The net weight gain is defined as the weight gain of the catalyst during the CH₃Cl pulse subtracted by the weight loss of the catalyst after CH₃Cl removal.

As the catalyst temperature increased from 400 °C to 700 °C, the weight gain due to CH₃Cl introduction decreased and the weight loss after CH₃Cl removal increased. Therefore, the net weight gain of the catalyst decreased as temperature increased. At 700 °C the net weight gain of the catalyst was zero, meaning that any species adsorbed during the CH₃Cl pulse was removed after CH₃Cl removal.

Carbon formation on a dry reforming catalyst is a common problem, which would also cause a weight gain of the catalyst. However, at these conditions carbon deposition is not expected thermodynamically because CO₂ is in excess of CH₄, therefore the species

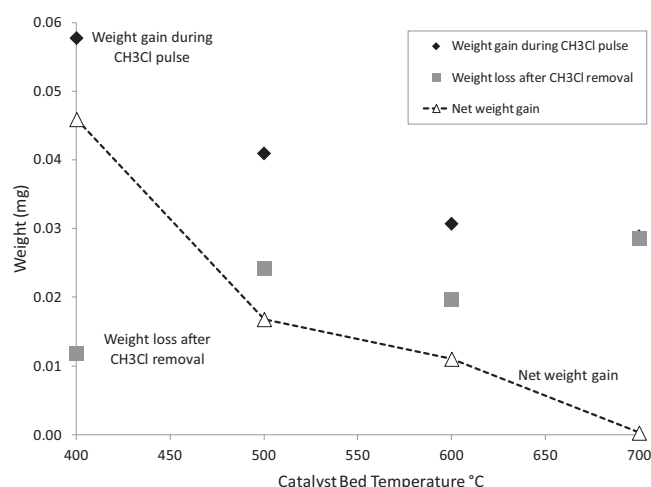


Fig. 6. Rh/γAl₂O₃ powder catalyst weight in mg as a function of temperature during and after 200 ppm CH₃Cl exposure in a feed of 5% CH₄, 6% CO₂, balance N₂.

causing the weight gain is not likely to be carbon, but either CH₃Cl or another chloride species. It is also important to note that precise quantitative comparisons cannot be made between this data and the flow-through reactor results because the flow dynamics are very different. In a TGA reactant gases flow over a sample pan or crucible containing catalyst powder, while in a flow-through reactor reactants are forced through the catalyst powder, encouraging greater contact between reactants and the catalyst surface. However, qualitative comparisons and trends can still be gleaned. At 400 °C the net weight gain of the catalyst is 0.046 mg, or 0.26 weight % of the Rh/γAl₂O₃ catalyst, while at 700 °C the net weight gain of the catalyst is 0.00 mg, indicating that the adsorption of this chloride species is favored at lower temperatures. This experiment was also performed for the Al₂O₃ support without impregnated rhodium at 400 °C; in this case the net weight gain of the alumina was 0.041 mg, or 0.22 weight %, similar to the weight gain on the Rh/γAl₂O₃ catalyst when exposed to CH₃Cl. This suggests that it

Table 4

Atom percent of surface species and assignments given using binding energies in Table 3.

XPS Peak	Assign-ment	400 °C No CH ₃ Cl 10 h	400 °C 50 ppm CH ₃ Cl 10 h	700 °C No CH ₃ Cl 3 h	700 °C 50 ppm CH ₃ Cl 3 h	700 °C No CH ₃ Cl 10 h	700 °C 50 ppm CH ₃ Cl 10 h
Al2p _A	Al ₂ O ₃	36.34	36.46	34.98	35.51	35.96	35.76
C1s _A	C _X	5.85	6.46	5.71	6.10	6.55	5.98
C1s _B	C _X	2.01	1.38	2.54	1.43	2.00	1.37
C1s _C	C _X	1.73	1.12	1.98	1.62	1.38	1.62
Cl2p _A	X-chloride	0.00	0.72	0.00	0.41	0.00	0.37
O1s _A	Al ₂ O ₃	53.50	53.07	54.18	54.30	53.43	54.19
Rh3d5 _A	Rh	0.00	0.17	0.00	0.00	0.33	0.00
	Rh ₂ O ₃	0.10		0.23	0.30		0.35
Rh3d5 _B	Rh ₂ O ₃	0.00	0.00	0.00	0.00	0.35	0.00
	Rh/AlO _X	0.57	0.61	0.37	0.33		0.37
	RhCl ₃	0.00		0.00		0.00	0.00

is the alumina support that is responsible for the chloride species adsorption on the Rh/ γ -Al₂O₃ catalyst.

3.3. XPS

X-ray photoelectron spectroscopy (XPS) was used to help determine the mechanism of CH₃Cl decomposition on the catalyst. Table 3 shows the orbital scans investigated and the peak binding energies determined for the elements shown, Al, Cl, O, and Rh in particular for each of the catalyst samples. Table 4 shows the assignments given to the elemental scans using known binding energies from the NIST XPS database [35] and literature [36,37] and the surface composition of the catalyst sample in atom percent.

There were two chemical species of rhodium present, referred to by subscripts “A” and “B.” Rh3d5_A resulted in binding energy peaks in the range of 307.8–308.3 eV, which may correspond to reduced elemental rhodium, Rh, or to rhodium oxide, Rh₂O₃. In general the binding energies are more characteristic of Rh₂O₃, but the ambiguous samples “400 °C, 50 ppm CH₃Cl, 10 h” and “700 °C, No CH₃Cl, 10 h” are illustrated in Table 4. The Rh3d5_B gave binding energy peaks in the range of 309.4–309.8 eV which may correspond to Rh₂O₃, Rh in a strong support interaction with the alumina, or rhodium chloride; RhCl₃. This ambiguity makes it difficult to determine in the chlorinated samples whether the Rh is associated with the chloride or only the aluminum oxide support. Again, the ambiguous cases, “400 °C, 50 ppm CH₃Cl, 10 h”, “700 °C, 50 ppm CH₃Cl, 3 h”, and “700 °C, No CH₃Cl, 10 h”, are noted in Table 4.

The Cl2p scan resulted in binding energy peaks ranging from 198.6 to 199.0 eV. Many chlorides lie in this range of binding energy, such as NaCl, KCl, K₂PtCl₄, RhCl₃, and alumina chloride species [36,37]. Because binding energies for RhCl₃ and alumina chloride species are similar, it is difficult to make a definitive assignment. However, if chloride was adsorbing on the rhodium, it is expected that this would cause a shift in the rhodium binding energies. In experiments comparing Pt and Pd catalysts freshly prepared with chlorinated precursors, which would leave adsorbed chloride on the metal, to the same catalysts reduced in H₂, which would remove the chloride from the metal, Karhu et al. noted a decrease in the Pt 4d_{5/2} or Pd 3d_{5/2} binding energies by 0.7–1.5 eV for the reduced catalysts [36]. When comparing the rhodium binding energies in Table 3 for samples exposed to CH₃Cl to those not exposed, there is no consistent shift in the rhodium spectrum. Therefore exposure to CH₃Cl does not seem to result in surface chloride that associates strongly with the rhodium metal.

There is a clear trend that more chloride is adsorbed on the catalyst surface at 400 °C compared to 700 °C. This is consistent with results from the TGA and flow-through reactor that suggested that chloride adsorption or poisoning decreases at higher temperatures. The XPS results also show that at the 700 °C 3 h and 10 h samples, the surface chloride concentrations were similar, 0.41 to 0.37 atom%, respectively. This indicates that chloride adsorption comes to equilibrium or saturates on the surface within 3 h, also confirmed with TGA experiments. This is also consistent with flow-through reactor results that show that the change in H₂/CO ratio due to CH₃Cl introduction occurs rapidly.

The XPS results confirm that chloride species are adsorbing on the catalyst as a result of CH₃Cl exposure during the dry reforming reaction. The location of these chloride species is not definitive, but the available data combined with literature results suggest that the chloride is associated with the alumina and not the rhodium metal. Furthermore, it is clear that chloride adsorption decreases with increasing temperature, which is consistent with the flow-through reactor and TGA results.

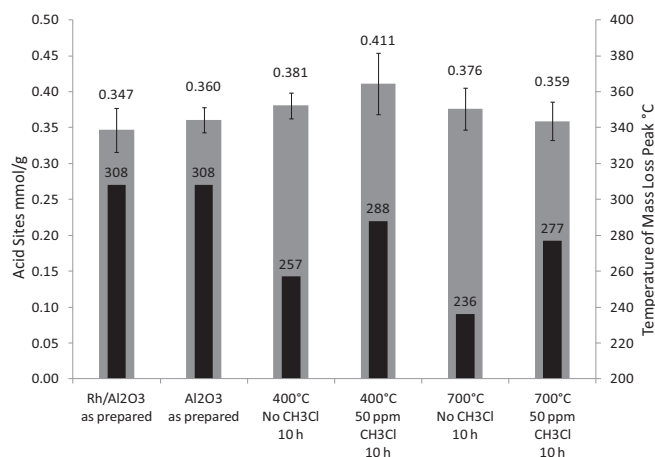


Fig. 7. Acidity in mmole/g on primary ordinate measured using NH₃ TPD of fresh and reacted 4% Rh/Al₂O₃ powder samples. Temperature at maximum rate of weight loss of Rh/Al₂O₃ catalyst samples during NH₃ desorption step on secondary ordinate. NH₃ adsorbed at 100 °C. Samples exposed to reaction conditions at stated temperatures (400 °C and 700 °C).

3.4. Acidity characterization

The six Rh/ γ -Al₂O₃ samples exposed to a dry reforming mixture with and without CH₃Cl for 3 or 10 h at 400 °C or 700 °C, shown in Table 1, as well as pre-tested samples of Rh/Al₂O₃ and Al₂O₃, were tested for the sum of Lewis and Brønsted acidity by ammonia temperature programmed desorption. Fig 7 shows the number of acid sites measured in millimole per gram of catalyst (mmol/g) and the relative strength of those acid sites on un-reacted Rh/Al₂O₃, Al₂O₃, and the catalyst samples reacted for 10 h. Fig. 7 shows that the number of acid sites on all samples ranged from 0.347–0.411 mmol/g catalyst. All samples exhibit the same approximate number of acid sites, except for the sample reacted with CH₃Cl at 400 °C, which may indicate that exposure to CH₃Cl increases the number of acid sites on the catalyst.

Fig. 7 also shows the temperatures at which the rate of NH₃ desorption from the catalyst was the highest for the six catalyst samples. This temperature is a measure of the acid site strength because NH₃ desorbed at higher temperatures would have been associated with stronger acid sites on the catalyst. As expected, the NH₃ desorption temperature for pre-tested Al₂O₃ and Rh/Al₂O₃ is the same because the acid strength of the catalyst originates from the alumina and is unaffected by the presence of small amounts of rhodium. However, for the catalyst samples exposed to a dry reforming feed for 10 h, CH₃Cl exposure increased the strength of acid sites on the catalyst, even at 700 °C. This provides evidence that exposure of the Rh/Al₂O₃ catalyst to CH₃Cl during the reforming reaction increases the strength of acid sites on a catalyst, even at the relatively high temperature of 700 °C at which the changes in activity and selectivity were subtle. Therefore, catalyst samples exposed to CH₃Cl at both 400 °C and 700 °C had an increase in the strength of acid sites, and at 400 °C the number of acid sites may have also increased. This result is consistent with literature, particularly from the field of naphtha reforming [6,38] in which chlorocarbons are used to maintain the acidity of naphtha reforming catalysts. This also further supports the hypothesis that chloride adsorption occurs on the alumina support, where the acidity and basicity of the Rh/Al₂O₃ catalyst originate.

4. Discussion

Flow-through reactor results showed that exposure of a Rh/ γ -Al₂O₃ catalyst to CH₃Cl while dry reforming CH₄ and CO₂

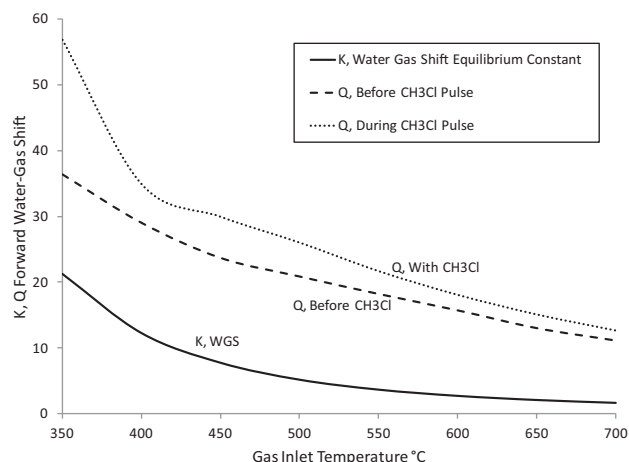


Fig. 8. K and Q for the water–gas shift reaction before and during exposure to 50 ppm CH_3Cl in a feed of 5.6% CH_4 and 7% CO_2 in a balance of N_2 on a 4% $\text{Rh}/\gamma\text{Al}_2\text{O}_3$ powder catalyst.

caused a change in product selectivity, particularly an increase in CO_2 and H_2 and a decrease in CO and H_2O in the products, producing syngas with a higher H_2/CO ratio. These changes appear to reflect a poisoning of the reverse water–gas shift reaction (Eq. (2)). After the CH_3Cl is removed, the H_2/CO ratio returns to its pre- CH_3Cl values, indicating that the poisoning of the reverse water–gas shift reaction due to CH_3Cl is reversible, also shown in Fig. 3 for every temperature except 350 °C. At 350 °C the effect of CH_3Cl may be partially irreversible, or require more time for regeneration.

It is important to note that at the temperature and space velocities achieved in these experiments, the water–gas shift reaction is not at equilibrium. This is shown by comparing the equilibrium constant, K (Eq. (6)), for the water–gas shift reaction to the reaction quotient, Q (Eq. (7)), calculated using the product species from the experiment shown in Figs. 2 and 3. K is calculated using equilibrium concentrations of H_2 , CO_2 , H_2O , and CO .

$$K, \text{WGS} = \frac{[\text{H}_2, \text{eq}][\text{CO}_2, \text{eq}]}{[\text{H}_2\text{O}, \text{eq}][\text{CO}, \text{eq}]} \quad (6)$$

$$Q, \text{WGS} = \frac{[\text{H}_2][\text{CO}_2]}{[\text{H}_2\text{O}][\text{CO}]} \quad (7)$$

The results of Q , calculated before and after the CH_3Cl pulse, and K are presented in Fig. 8. At all temperatures the reaction quotient before CH_3Cl introduction is greater than the equilibrium constant, meaning that the water–gas shift reaction is not at equilibrium and the reaction potential is toward the reverse water–gas shift direction. The reaction quotient increased when CH_3Cl was introduced, meaning that the reverse water–gas shift reaction moved farther from equilibrium and was therefore likely poisoned by CH_3Cl . After the CH_3Cl was removed Q returned to its pre- CH_3Cl value at each temperature (not plotted), further supporting that the reverse water–gas shift poisoning is reversible.

The cause of the reverse water gas shift poisoning may be chloride deposition on the catalyst. XPS results confirmed that chloride remained on the catalyst, likely the alumina support, after CH_3Cl exposure during the dry reforming reaction. The amount of chloride present decreased with temperature. This was consistent with TGA results that showed that the weight gain of the catalyst as a result of CH_3Cl exposure decreased with temperature, and flow-through reactor results showing that the effect of CH_3Cl on the H_2/CO ratio is inversely proportional to temperature. Flow-through reactor results also showed that the change in selectivity is directly proportional to CH_3Cl concentration and that introduction of HCl

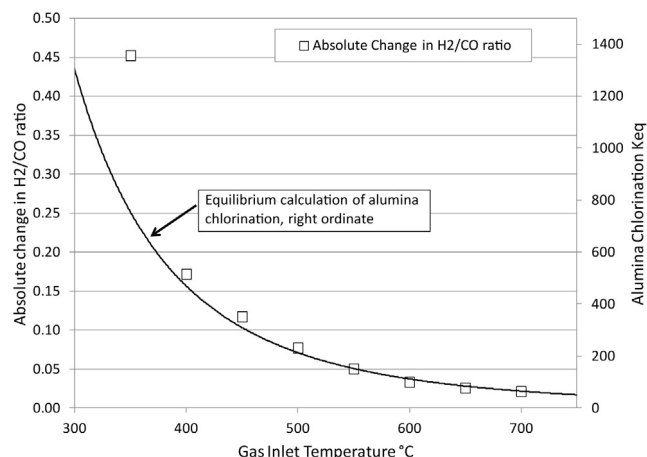


Fig. 9. Absolute change in H_2/CO ratio as a function of temperature as a result of 50 ppm CH_3Cl exposure in a feed of 5.6% CH_4 and 7% CO_2 in a balance of N_2 . Keq, equilibrium constant of alumina chlorination reaction, as a function of temperature calculated using Castro model.

in the dry reforming reaction elicited the same changes in H_2/CO as CH_3Cl , indicating that HCl or chloride is the key poisoning species.

Furthermore, thermo-gravimetric analysis showed that the alumina support experienced the same weight gain when exposed to CH_3Cl as the $\text{Rh}/\gamma\text{Al}_2\text{O}_3$ catalyst. This provides another indication that the alumina support is primarily responsible for the chloride species adsorption. Also, acidity characterization revealed that CH_3Cl exposure increased catalyst acidity, which generally originates from the alumina support. These results suggest a mechanism by which CH_3Cl reacts on the catalyst, leaving chloride on the alumina support, which increases the acidity of the catalyst and poisons the reverse water–gas shift reaction.

In light of the flow through reactor and characterization results, a likely cause of the reverse water–gas shift poisoning is the replacement of alumina hydroxyl groups by chloride, as illustrated in Eq. (5). Castro et al.'s model [24,25] for naphtha reforming assumes that chlorination occurs by this mechanism. Castro determined the equilibrium constant of this reaction as a function of temperature using various mixtures of H_2O and HCl on $\gamma\text{Al}_2\text{O}_3$ and $\text{Pt}/\gamma\text{Al}_2\text{O}_3$ catalysts at various temperatures [25]. It was determined that the equilibrium constant, and therefore chlorination of the alumina, is primarily a function of the reaction temperature and the $\text{H}_2\text{O}/\text{HCl}$ ratio in the feed.

This model was applied to the flow-through reactor results presented here to assess the validity of the model on the 4% $\text{Rh}/\gamma\text{Al}_2\text{O}_3$ catalyst. The equilibrium constant, K , for the reaction shown in Eq. (5), was calculated for the range of temperatures between 300 °C and 800 °C and plotted on the secondary ordinate in Fig. 9. Experimental results showing the change in H_2/CO ratio as a result of a 1 h CH_3Cl pulse during the dry reforming reaction are plotted on the primary ordinate in Fig. 9. These values are calculated from the data in Fig. 3 by subtracting the H_2/CO ratio during the CH_3Cl pulse from the H_2/CO ratio before CH_3Cl introduction.

As temperature increases, the alumina chlorination equilibrium constant decreases, resulting in more alumina hydroxyl groups and gas-phase HCl , as opposed to chlorinated alumina and H_2O , according to Eq. (5). In other words, at high temperatures, the chlorination of the alumina support is not thermodynamically favored. Because chloride replaces alumina hydroxyl groups that participate in the forward and reverse water–gas shift reactions, less chlorination will result in less reverse water–gas shift poisoning, and will therefore produce a smaller change in the H_2/CO ratio when CH_3Cl is introduced into the dry reforming feed. This provides an

explanation for why the change in product selectivity, illustrated by the H_2/CO ratio, decreases as temperature increases.

While steam reforming chlorocarbons over a range of catalysts, Richardson et al. noted a poisoning of the forward water–gas shift reaction, Eq. (3). According to Eq. (5), the H_2O introduced for the steam reforming reaction should keep the surface free of chloride adsorption. However, according to the Castro model [24,25], the degree of alumina chlorination is a function on the H_2O/HCl ratio, not the absolute amount of H_2O or chlorinated compound in the feed. Assuming that chlorocarbons either decompose to HCl or leave chloride on the surface in a way similar to HCl , the H_2O/Cl ratio can be calculated and used for comparison rather than the H_2O/HCl ratio. In the chlorocarbon steam reforming experiments of Richardson et al., the H_2O/Cl ratio ranged from 6.5 to 20 [14,15,17,18,20]. In this work, while the CH_3Cl concentration was low, the H_2O concentration was also low because it was produced by the reverse water–gas shift reaction and not added to the feed. The H_2O/Cl ratio in the experiments presented here was 46.5 for 50 ppm CH_3Cl . This explains why poisoning of the forward water–gas shift reaction was still observed in chlorocarbon steam reforming experiments: while H_2O was abundant, the H_2O/Cl ratio was low.

The direction of the water–gas shift poisoning is a function of the reaction conditions. In Richardson's chlorocarbon steam reforming work, the forward water–gas shift reaction was poisoned. The equilibrium constant K (Eq. (6)) and reaction quotient Q (Eq. (7)) for the water–gas shift reaction were calculated for CH_3Cl steam reforming conditions and it was determined that at temperatures between 400 °C and 750 °C, Q was less than K , meaning that the forward water–gas shift reaction was not at equilibrium due to poisoning by CH_3Cl [20]. In this work, the reverse water–gas shift reaction is poisoned because, as previously illustrated, the reaction was not at equilibrium with a potential toward the reverse direction due to the abundance of CO_2 and absence of H_2O in the feed. Because chloride adsorption removes alumina hydroxyl groups which are required to produce the necessary formate or carbonate intermediates [28–33] in both the forward and reverse water–gas shift reactions, both directions can be poisoned, depending on the conditions. In this case, abundant in CO_2 and operating far from equilibrium, the reverse water–gas shift reaction was poisoned by chloride adsorption.

An open question is how CH_3Cl supplies chloride to the alumina support. It is possible that the CH_3Cl reacts on the metal surface by a step-wise dechlorination and dehydrogenation, similar to the proposed mechanism by Wei and Iglesia for CH_4 reforming that proceeds via a step-wise dehydrogenation [39–42]. Because the bond dissociation energy of a CH_3-H bond is higher than that of a CH_3-Cl bond [43], it is likely that the $C-Cl$ bond will break with less energy input than the $C-H$ bonds. The initial breaking of the $C-Cl$ bond as a rate limiting step in hydrodechlorination is observed in other work [44–47]. This stepwise dehydrogenation would produce H^* that later forms H_2 , surface C^* that is oxidized to CO in a later step, and surface chloride. The surface chloride may then migrate from the metal to the support, similar to the way H^* spills over from the metal to the support, or chloride may react with gas phase hydrogen to form HCl which then reacts with the alumina support.

In order for the chloride to move from the metal to the support via spill-over, there must be sufficient OH groups around the perimeter of the rhodium to react with the chloride to produce aluminum chloride and H_2O , as proposed in Eq. (5). The number of OH groups can be calculated using Eq. (8):

$$I_o = \alpha * X_m * D^2 \quad (8)$$

where I_o is the specific perimeter of the rhodium in units of m/g catalyst, α is the perimeter of one particle of rhodium in units of m/g catalyst, X_m is the metal loading in %, and D is the dispersion of the

metal in %. α is assumed to be 8.8×10^5 m/g, assuming hemispherical particles of rhodium [29], X_m is 4%, and D is 40%. This produces an I_o of 3.83×10^9 m/g catalyst. Assuming the distance between OH groups is 2 \AA [48], the concentration of OH groups around the periphery of the rhodium particles is $47.3 \text{ } \mu\text{mol/g}$. According to the XPS results, the amount of chloride adsorbed on the catalyst after 10 h exposure to a feed of 5.6% CH_4 , 7% CO_2 and 50 ppm CH_3Cl in a balance of N_2 at 400 °C is 1.25 wt%, or $352 \text{ } \mu\text{mol/g}$. Therefore the amount of chloride adsorbed on the alumina surface from the CH_3Cl is an order of magnitude greater than the number of OH groups around the periphery of the rhodium particles, so the chloride must not rely only on spill-over from the metal to the support to reach the alumina support, unless the chloride can easily migrate throughout the alumina.

For the chloride to form HCl , it must react with H^* which is abundant on the metal due to the CH_4 and CH_3Cl dehydrogenation reactions. The gas phase HCl is then mobile and may react with the alumina support to form aluminum chloride species on the surface. Flow-through reactor experiments showed that the effect of HCl on Rh/Al_2O_3 was similar to the effect of CH_3Cl . Therefore HCl does clearly interact with the catalyst surface and it is possible that HCl is the species responsible for the poisoning of the alumina.

Either explanation for how CH_3Cl provides chloride to the alumina support is currently plausible. Future experimental and computational work to determine the activation energies and reaction rates of the elementary steps involved in chlorocarbon decomposition and reforming would allow for the incorporation of the chlorocarbon reactions into pre-existing micro-kinetic models, which could provide another diagnostic tool to determine the effect of chlorocarbons on the reforming of CH_4 and other fuels.

5. Conclusions

Biogas is an inexpensive energy source but has a low heating value due to its high CO_2 content. The gas can be upgraded using catalytic dry reforming, but the presence of CH_3Cl and other chlorocarbons in 10–50 ppm concentrations have the potential to poison the catalyst. It was determined here that chloride from CH_3Cl adsorbs on the alumina support during the dry reforming reaction over a $Rh/\gamma-Al_2O_3$ catalyst increasing the acidity of the support. This leads to reversible poisoning of the reverse water–gas shift reaction. The amount of chloride adsorption and poisoning is proportional to the concentration of CH_3Cl . Chlorination of alumina is less thermodynamically favored at high temperatures and therefore the amount of chloride adsorbed decreases as temperature increases.

Chloride adsorption poisons the reverse water–gas shift reaction, which increases the H_2/CO ratio of the syngas, by replacing hydroxyl groups on the alumina support which are intermediates in both the forward and reverse water–gas shift reactions. Introduction of HCl instead of CH_3Cl under the same reaction conditions causes the same changes in selectivity as CH_3Cl , indicating that the chloride reaction mechanism is similar. It has been shown that the acid-base pairs on the alumina are attacked by HCl to adsorb chloride [23]. Therefore, a support with less acidity or fewer acid-base pairs would be less vulnerable to chloride poisoning. A ZrO_2 support which has fewer acidic and basic sites has been shown in other work to resist chloride poisoning during the steam reforming of CH_3Cl [22]. For chlorocarbon reforming applications in which chloride adsorption is not desired, catalyst supports with less acidity may be effective.

In summary, the amount of chlorocarbon expected in a biogas mixture, between 10 and 50 ppm, is not an irreversible poison for the 4% Rh/Al_2O_3 catalyst. The most noticeable effect of chloride adsorption is a change in H_2/CO ratio of the syngas that

is proportional to the amount of chlorocarbon in the feed. The effect is completely and quickly reversible after the chlorocarbon is removed. A higher H_2/CO ratio may even be desirable in some operations. Process conditions can also be modified to reduce chloride adsorption, for example H_2O co-feeding or operation at temperatures above $500^\circ C$.

Acknowledgements

The authors would like to thank the Combustion and Catalysis Laboratory at Columbia University, Columbia University Presidential Fellowship, and BASF-Columbia Research Partnership for supporting this research. Thank you to Nancy Brungard for her help obtaining and interpreting the XPS data.

References

- [1] EPA, Landfill Methane Outreach Program, 2011.
- [2] P. Simmons, N. Goldstein, S. Kaufman, N.J. Themelis, J. Thompson, *BioCycle* 1 (2006) 26–43.
- [3] N.J. Themelis, P.A. Ulloa, *Renewable Energy* 32 (2007) 1243–1257.
- [4] M.P. Kohn, J. Lee, M.L. Basinger, M.J. Castaldi, *Industrial & Engineering Chemistry Research* 50 (2011) 3570–3579.
- [5] M.P. Kohn, M.J. Castaldi, R.J. Farrauto, *Applied Catalysis B-Environmental* 94 (2010) 125–133.
- [6] R.J. Farrauto, C. Bartholomew, *Fundamentals of Industrial Catalytic Processes*, second ed., John Wiley & Sons; American Institute of Chemical Engineers, Portland, Oregon, 2006.
- [7] J. Rostrup-Nielsen, J.H.B. Hansen, *Journal of Catalysis* 144 (1993) 38–49.
- [8] G. Tchobanoglous, H. Theisen, S. Vigil, *Integrated Solid Waste Management*, McGraw-Hill, New York, 1993, Print.
- [9] N. Whitmore, in: M. Castaldi (Ed.), *Landfill Gas Constituents*, 2004.
- [10] J.T.G. Hamilton, W.C. McRoberts, F. Keppler, R.M. Kalin, D.B. Harper, *Science* 301 (2003) 206–209.
- [11] J. Bao, G.N. Krishnan, P. Jayaweera, J. Perez-Mariano, A. Sanjurjo, *Journal of Power Sources* 193 (2009) 607–616.
- [12] W.C. Keene, M.A.K. Khalil, D.J. Erickson, A. McCulloch, T.E. Graedel, J.M. Lobert, M.L. Aucott, S.L. Gong, D.B. Harper, G. Kleiman, P. Midgley, R.M. Moore, C. Seuzaret, W.T. Sturges, C.M. Benkovitz, V. Koropalov, L.A. Barrie, Y.F. Li, *Journal of Geophysical Research-Atmospheres* 104 (1999) 8429–8440.
- [13] A. McCulloch, M.L. Aucott, C.M. Benkovitz, T.E. Graedel, G. Kleiman, P.M. Midgley, Y.F. Li, *Journal of Geophysical Research-Atmospheres* 104 (1999) 8391–8403.
- [14] N. Coute, J.D. Ortego, J.T. Richardson, M.V. Twigg, *Applied Catalysis B-Environmental* 19 (1998) 175–187.
- [15] N. Coute, J.T. Richardson, *Applied Catalysis B-Environmental* 26 (2000) 265–273.
- [16] N. Coute, J.T. Richardson, *Applied Catalysis B-Environmental* 26 (2000) 217–226.
- [17] K. Intarajang, J.T. Richardson, *Applied Catalysis B-Environmental* 22 (1999) 27–34.
- [18] T.E. McMin, F.C. Moates, J.T. Richardson, *Applied Catalysis B-Environmental* 31 (2001) 93–105.
- [19] F.C. Moates, T.E. McMin, J.T. Richardson, *AIChE Journal* 45 (1999) 2411–2418.
- [20] J.D. Ortego, J.T. Richardson, M.V. Twigg, *Applied Catalysis B-Environmental* 12 (1997) 339–355.
- [21] J.T. Richardson, J.D. Ortego, N. Coute, M.V. Twigg, *Catalysis Letters* 41 (1996) 17–20.
- [22] M. Shafiei, J.T. Richardson, *Applied Catalysis B-Environmental* 54 (2004) 251–259.
- [23] E. Santacesaria, D. Gelosa, S. Carra, *Industrial & Engineering Chemistry Product Research and Development* 16 (1977) 45–47.
- [24] A.A. Castro, O.A. Scelza, G.T. Baronetti, M.A. Fritzler, J.M. Parera, *Applied Catalysis* 6 (1983) 347–353.
- [25] A.A. Castro, O.A. Scelza, E.R. Benvenuto, G.T. Baronetti, J.M. Parera, *Journal of Catalysis* 69 (1981) 222–226.
- [26] M. Digne, P. Raybaud, P. Sautet, D. Guillaume, H. Toulhoat, *Journal of the American Chemical Society* 130 (2008) 11030–11039.
- [27] J.C. Musso, J.M. Parera, *Applied Catalysis* 30 (1987) 81–90.
- [28] R. Burch, *Physical Chemistry Chemical Physics* 8 (2006) 5483–5500.
- [29] D. Martin, D. Duprez, *Journal of Physical Chemistry B* 101 (1997) 4428–4436.
- [30] D. Martin, D. Duprez, *Journal of Physical Chemistry* 100 (1996) 9429–9438.
- [31] K. Tanabe, M. Misono, Y. Ono, H. Hattori, *New Solid Acids and Bases*, Elsevier, Tokyo, 1989.
- [32] C. Morterra, G. Magnacca, *Catalysis Today* 27 (1996) 497–532.
- [33] H. Knozinger, P. Ratnasamy, *Catalysis Reviews – Science and Engineering* 17 (1978) 31–70.
- [34] G. Bergeret, P. Gallezot, *Handbook of Heterogeneous Catalysis*, Wiley-VCH Verlag GmbH & Co. KGaA, 2008.
- [35] C.D. Wagner, A.V. Naumkin, A. Kraut-Vass, J.W. Allison, C.J. Powell, J.R. Rumble Jr., *NIST X-ray Photoelectron Spectroscopy Database*, 2007.
- [36] H. Karhu, A. Kalantar, I.J. Vayrynen, T. Salmi, D.Y. Murzin, *Applied Catalysis a – General* 247 (2003) 283–294.
- [37] I. Bennour, V. Maurice, P. Marcus, *Surface and Interface Analysis* 42 (2010) 581–587.
- [38] L. Lloyd, *Handbook of Industrial Catalysis*, Springer, New York, 2011.
- [39] J.M. Wei, E. Iglesia, *Physical Chemistry Chemical Physics* 6 (2004) 3754–3759.
- [40] J.M. Wei, E. Iglesia, *Journal of Catalysis* 224 (2004) 370–383.
- [41] J.M. Wei, E. Iglesia, *Journal of Catalysis* 225 (2004) 116–127.
- [42] J.M. Wei, E. Iglesia, *Abstracts of Papers of the American Chemical Society*, vol. 227, 2004, pp. U1072–U1072.
- [43] W.M. Haynes, D.R. Lide (Eds.), *CRC Handbook of Chemistry and Physics*, 2012.
- [44] B. Coq, G. Ferrat, F. Figueras, *Journal of Catalysis* 101 (1986) 434–445.
- [45] Y. Hashimoto, Y. Uemichi, A. Ayame, *Applied Catalysis a – General* 287 (2005) 89–97.
- [46] N. Chen, R.M. Rioux, L. Barbosa, F.H. Ribeiro, *Langmuir* 26 (2010) 16615–16624.
- [47] P. Choudhury, J.K. Johnson, *Journal of Physical Chemistry C* 115 (2011) 11694–11700.
- [48] G.G. Olympiou, C.M. Kalamaras, C.D. Zeinalipour-Yazdi, A.M. Efstathiou, *Catalysis Today* 127 (2007) 304–318.